

Available online at [www.sciencedirect.com](http://www.sciencedirect.com)**SciVerse ScienceDirect**

Procedia Environmental Sciences 18 (2013) 478 – 485

**Procedia**

Environmental Sciences

2013 International Symposium on Environmental Science and Technology (2013 ISEST)

## Photocatalytic Degradation of Methyl Orange with Commercial Organic Pigment Sensitized TiO<sub>2</sub>

Xili Shang<sup>a,b</sup>, Bin Li<sup>a,\*</sup>, Tianyong Zhang<sup>a,\*</sup>, Changhai Li<sup>b</sup>, Xiao Wang<sup>a</sup><sup>a</sup>*School of Chemical Engineering and Technology, Tianjin University, Tianjin 300072, China*<sup>b</sup>*Department of Chemistry and Chemical Engineering, Binzhou University, Binzhou 256603, China*

### Abstract

In this paper, TiO<sub>2</sub> photocatalyst sensitized with commercial organic pigment, C.I. Pigment Yellow 154 (PY) or C.I. Pigment Red 254 (PR) was prepared by solvothermal method, respectively. Photocatalytic activities of the as-prepared pigment/TiO<sub>2</sub> composites was evaluated by the degradation of the methyl orange (MO) under visible light irradiation. Microstructural, morphological, and optical properties of the as-prepared pigment/TiO<sub>2</sub> composites were characterized by X-ray diffraction technique (XRD), BET surface area analysis, UV–vis diffuse reflectance spectrum (UV–vis DRS). Results displayed that the as-prepared pigment/TiO<sub>2</sub> composites have high visible light photocatalytic activity and stability. The TOF of pigment/TiO<sub>2</sub> based on the content of pigment had nearly loss when the photocatalyst was used four times. The remarkable enhancement in the visible light photocatalytic activities of the pigment/TiO<sub>2</sub> heterostructures could be attributed to the effective electron–hole separations at the interfaces of the two semiconductors.

© 2013 The Authors. Published by Elsevier B.V. Open access under [CC BY-NC-ND license](#).  
Selection and peer-review under responsibility of Beijing Institute of Technology.

**Keywords:** Commercial organic pigment; Methyl orange; TiO<sub>2</sub>; Photocatalysis; Visible light

### 1. Introduction

Titanium dioxide as a photocatalyst for mineralization of organic pollutants has attracted much attention because of its various advantages [1]. However, the large band-gap energy (3.2 eV) of TiO<sub>2</sub> considerably limits the utilization of natural solar light or artificial visible light [2]. As a surface modification technology, dye sensitization can be effective in broadening the range of semiconductor absorption [3, 4]. The properties of the dye play an important role in determining semiconductor photocatalytic performance. Due to the aqueous solubility of dye [5], the dye sensitized TiO<sub>2</sub> will easily

\* Corresponding Author. Tel & fax: +00-86-22-27406610.  
E-mail address: tyzhang@tju.edu.cn (TY Zhang).

and frequently lose visible light activity in the course of photocatalytic degradation of organic pollutants[6].

In response to this defect, we selected special commercial stable pigment as sensitizer because of its high absorption coefficient within the solar spectrum and insoluble properties in water. C.I.Pigment Yellow 154 (PY) made in China, a commercial pigment with benzimidazolone azo group, is often used as automobile coatings because of its notable stability, weather resistance and solvent resistance. C.I.Pigment Red 254 (PR) is often used for printing inks, plastic, paint and coating because of its high colour strength, excellent heat and light resistance. Fig. 1 illustrates molecular structure of PY and PR. In this study, PY and PR sensitized  $\text{TiO}_2$  (labelled as PY/ $\text{TiO}_2$  and PR/ $\text{TiO}_2$  respectively) photocatalysts were prepared by solvothermal method. The photocatalytic activity and stability of PY/ $\text{TiO}_2$  were evaluated on the degradation of methyl orange (MO) under visible light irradiation.

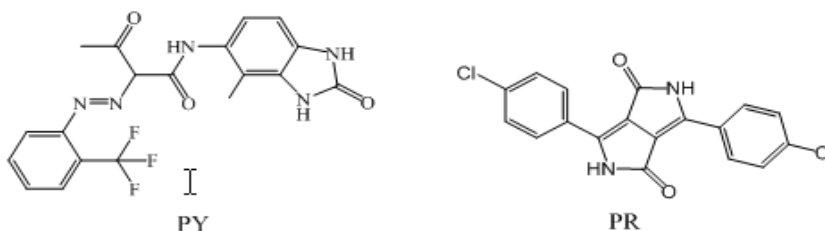


Fig. 1. Molecular structure of PY and PR.

## 2. Experimental

### 2.1. Materials and preparation of PY/ $\text{TiO}_2$ and PR $\text{TiO}_2$

The modified  $\text{TiO}_2$  with PY (PY/ $\text{TiO}_2$ ) was prepared by solvothermal method as follows. A mixture of PY (1.1 mmol), Span 80 (0.5 mmol) and DMF (80 mL) were sealed in a 100 mL Teflon-lined sealed reactor and heated in an oven at 150 °C. After 0.5 h the resultant mixture was filtered hot to remove trace amounts of insoluble solids and obtain solution A. 4.14 g  $\text{TiO}_2$  (P25, 51.8 mmol) was dispersed in approximately 20 mL of DMF under ultrasonic vibrations at room temperature for 10 min to obtain white slurry B. Solution A and slurry B were diverted into a 125 mL Teflon-lined sealed reactor and heated in an oven at 195 °C for 4 h, and then slowly cooled to room temperature. After filtration, the resulting powder was washed with distilled deionized water and ethanol several times and dried at 80 °C in oven to obtain a yellowish powder of PY/ $\text{TiO}_2$  photocatalyst (4.38 g), and proved that 54% of original PY was deposited onto  $\text{TiO}_2$ . PR/ $\text{TiO}_2$  was prepared as the same method and the dosage of reactants were the same also, and 48% of original PR was deposited onto  $\text{TiO}_2$ . The contents of organic pigment in catalysts (PY/ $\text{TiO}_2$  and PR/ $\text{TiO}_2$ ) are 5.5% and 4.4% for PY and PR respectively.

### 2.2. Characterizations of PY/ $\text{TiO}_2$ and PR $\text{TiO}_2$

To determine the crystal phase composition of as-prepared photocatalysts, X-ray diffraction (XRD) measurements were carried out using a X'Pert Pro X-ray diffractometer (PANAAlytical, Holland) with Cu  $K\alpha$  radiation, the diffractograms were recorded in the  $2\theta$  range 10°–80° with steps of 0.017°. The surface

physical morphology of the photocatalysts was measured by nitrogen adsorption isotherms at  $-196\text{ }^{\circ}\text{C}$  by using a Micromeritics Tristar II 3020 system (Micromeritics Instrument Corporation, America). UV–Vis diffuse reflectance spectra were performed using a PerkinElmer Lambda 750 spectrophotometer (Perkin Elmer Corporation, America).

### 2.3. Measurements of adsorption capacities and photocatalytic activities

The experiments were carried out in a custom-made adsorption-photodegradation reactor. The reactor consists of a 120 mL Pyrex glass bottle with a jacket outside and a 150 W tungsten iodine lamp in parallel to the reactor. To ensure the experiments were carried out under visible light, the light beam was passed through optical filter (JB420, Jiangsu Haian Education Optical Lens Factory, China) to cut-off wavelengths shorter than 420 nm. The photocatalytic activity of the as-prepared photocatalysts was evaluated by degradation of MO. Reaction suspensions were prepared by adding different photocatalysts to 100 mL MO solution (Initial concentration:  $8.3 \times 10^{-5}$  mol/L, catalyst dose 0.6 g/L) under vigorous stirring. The samples were collected at regular intervals of time and analyzed by Agilent 8453 UV–Vis spectrometer to measure the temporal changes of solution concentration. The concentration of MO was calculated by its calibration curve.

## 3. Results and discussion

### 3.1. Characterization of photocatalysts

#### 3.1.1. XRD patterns

The XRD patterns of the original  $\text{TiO}_2$ ,  $\text{PR/TiO}_2$  and  $\text{PY/TiO}_2$  are shown in Fig. 2. The original  $\text{TiO}_2$  exhibits typical patterns that can be well indexed to the phases of anatase and rutile. The modification of  $\text{TiO}_2$  by pigment PY or PR does not cause obvious change in their peak positions and shapes compared with the original  $\text{TiO}_2$ , which indicating that the sensitization of  $\text{TiO}_2$  through solvothermal treatment has not changed the crystalline structure of original  $\text{TiO}_2$ .

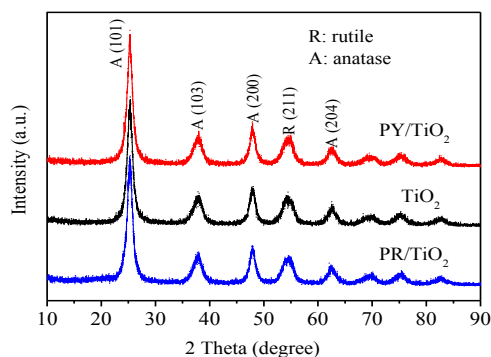


Fig. 2. XRD patterns of  $\text{TiO}_2$ ,  $\text{PY/TiO}_2$  and  $\text{PR/TiO}_2$ .

#### 3.1.2. $\text{N}_2$ Adsorption

The specific surface areas, average pore size and pore volume of the original  $\text{TiO}_2$  and as-prepared

photocatalysts were characterized using the  $N_2$  adsorption-desorption technique. Fig. 3 shows the  $N_2$  adsorption-desorption isotherms for PY/TiO<sub>2</sub>, PR/TiO<sub>2</sub> and TiO<sub>2</sub>. Table 1 summarizes their physical properties. The TiO<sub>2</sub> modified by PY or PR are aggregated to some extent during solvothermal treatment, leading to a marked decrease of the *BET* surface areas and the pore volume, and a marked increasing of the average pore size.

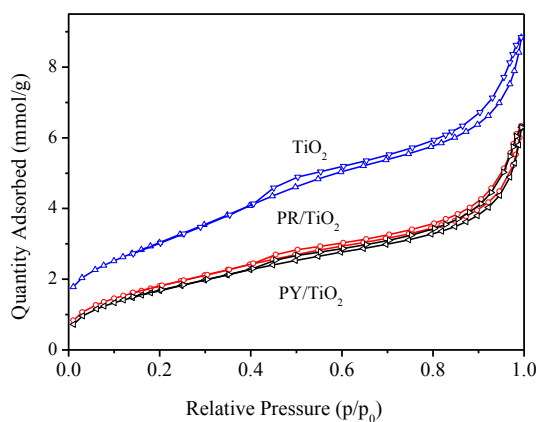


Fig. 3.  $N_2$  adsorption and desorption isotherms of TiO<sub>2</sub>, PR/TiO<sub>2</sub> and PY/TiO<sub>2</sub>.

Table 1. Structural characteristic of TiO<sub>2</sub> and PY/TiO<sub>2</sub>.

	Specific surface area (m <sup>2</sup> /g)	Pore volume (cm <sup>3</sup> /g)		Pore size (nm)	
	$S_{BET}$	$V_{BJH-A}$	$V_{BJH-D}$	$PS_{BJH-A}$	$PS_{BJH-D}$
TiO <sub>2</sub>	21.85	0.3314	0.3293	51.23	49.53
PY/TiO <sub>2</sub>	14.77	0.2304	0.2297	62.29	60.8
PR/TiO <sub>2</sub>	14.34	0.2333	0.2325	60.23	58.96

$S_{BET}$  = BET surface area;

$V_{BJH-A}$  = BJH adsorption cumulative volume of pores;

$V_{BJH-D}$  = BJH desorption cumulative volume of pores between 17 nm and 3000 nm width;

$PS_{BJH-A}$  = BJH adsorption average pore size;  $PS_{BJH-D}$  = BJH desorption average pore size.

### 3.1.3. UV-Vis diffuse reflectance spectra

Fig. 4 shows the UV-Vis diffuse reflectance spectra (UV-vis DRS) of PY/TiO<sub>2</sub>, PR/TiO<sub>2</sub> and original TiO<sub>2</sub>. Obviously, there was no absorption above 400 nm for pure TiO<sub>2</sub>, while PY/TiO<sub>2</sub> and PR/TiO<sub>2</sub> show clear visible light absorption from 400 to 600 nm. Approximately, the absorption edges of original TiO<sub>2</sub>, PY/TiO<sub>2</sub> and PR/TiO<sub>2</sub> are located at 382, 529 and 610 nm in the near-UV and visible light regions, respectively.

The reduction in the band gap energy of the as-prepared sample was determined by the following equation [7]:

$$E_g = \frac{1240}{\lambda} \quad (1)$$

where  $E_g$  is the band gap energy (eV) and  $\lambda$  is the wavelength (nm) of the absorption edge in the spectrum. Accordingly, the band gap of PY and PR are evaluated to be 2.34 eV and 2.03 eV, hence they can be excited by visible light ( $\lambda > 400$  nm,  $E_g < 3.1$  eV), whereas the band gap of  $\text{TiO}_2$  is found to be about 3.25 eV.

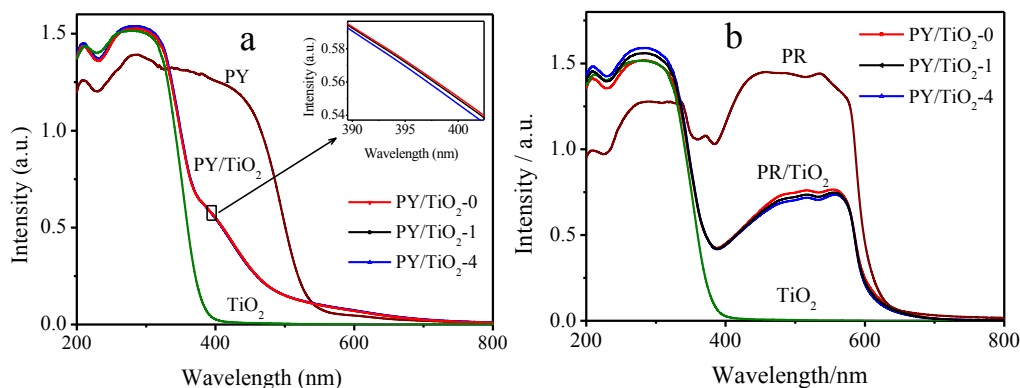


Fig. 4. UV-Vis diffuse reflectance spectra. (a) PY, PY/ $\text{TiO}_2$  and  $\text{TiO}_2$ ; (b) PR, PR/ $\text{TiO}_2$  and  $\text{TiO}_2$ . -0, -1, -4 are the number of cycle of the catalyst used for photocatalytic experiment.

### 3.2. Photocatalytic activity

MO, a stable acid azo dye, is a compound that contain azo groups ( $-\text{N}=\text{N}-$ ) linked to aromatic  $\text{sp}^2$ -hybridized C-atoms. MO is commonly used as titration indicator and staining agent in view of its high stability. In this paper, we investigated the photocatalytic activity of the prepared photocatalyst on the degradation of MO.

Fig. 5 shows UV-Vis spectral changes of MO aqueous solution in the presence of PY/ $\text{TiO}_2$ . Photocatalytic reaction started after 65 min of adsorption in the dark, the adsorption equilibrium had been established. The peak wavelength of MO aqueous solution clearly blue-shifted to the shorter range and simultaneously broaden under visible light irradiation, which is caused by *N*-demethylation according with the study reported by Zhu et al. [8], Han et al. [9] and Zhu et al. [10].

The changes in the concentration of MO aqueous solution under visible light irradiation in the presence of different photocatalysts are illustrated in Fig. 6. The degradation rate reached 89.2% and 50.9% respectively in 195 min. It is notable that PY/ $\text{TiO}_2$  and PR/ $\text{TiO}_2$  showed higher photocatalytic activities than pure  $\text{TiO}_2$ .

### 3.3. Turnover frequency (TOF) and recycle ability of the catalyst

The catalyst turnover number (*TON*) and the turnover frequency (*TOF*) are two important quantities used for comparing catalyst efficiency. In heterogeneous catalysis, the *TON* is the number of reactant molecules that is converted into products in presence of 1 g of catalyst [11]. The *TOF* is simply *TON*/time. For pigment/ $\text{TiO}_2$  catalyst using MO solution (Initial concentration: 27 mg/L) and 0.6 g/L catalyst dose, the *TOF* based on the content of pigment were found to be  $5.9 \times 10^{-7}$  and  $3.8 \times 10^{-7}$  molecules/g/min for the first cycle for PY/ $\text{TiO}_2$  and PR/ $\text{TiO}_2$  respectively.

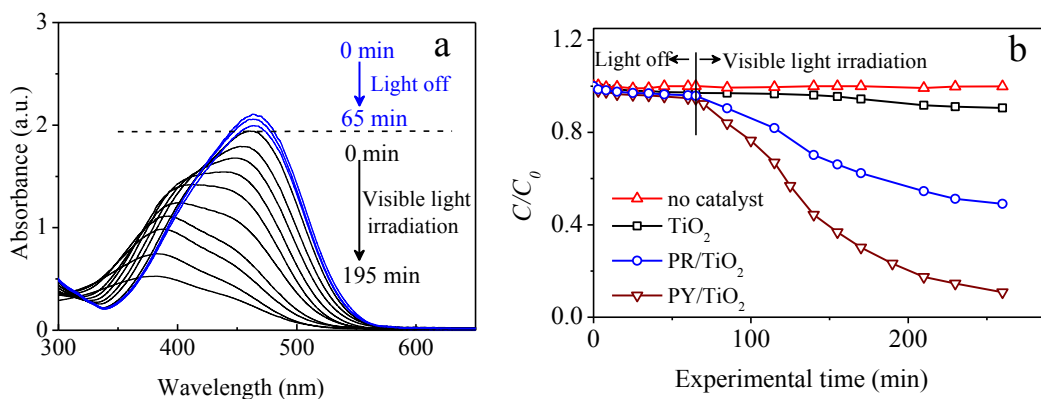


Fig. 5. (a) Temporal spectral changes of MO in aqueous PY/TiO<sub>2</sub> suspensions under visible light irradiation, (b) Photodegradation of MO under different photocatalysts.

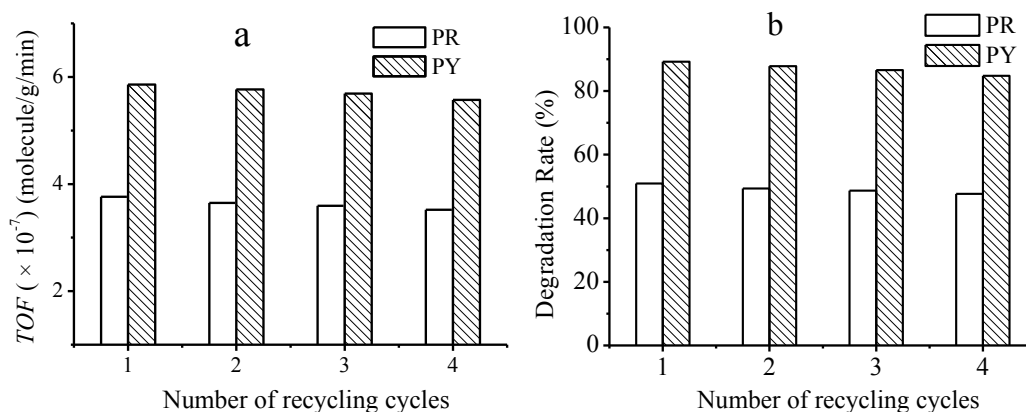


Fig. 6. (a) TOF, and (b) MO photodegradation at successive catalytic cycles. Concentration of MO: 27 mg/L; Catalyst dose: 0.6 g/L; Irradiation time: 195 min.

To make the process cost-effective and greener, the recycle ability of pigment/TiO<sub>2</sub> was evaluated. After completion of one catalytic cycle, the used photocatalyst was collected by filtrating the suspension and washed with distilled deionized water to remove the bulk solution, dried in oven at 100 °C for 0.5 h. There is little loss of photocatalytic activity observed when the photocatalyst was used four times (Fig. 6), which illustrate that the content of pigment in catalyst has nearly change, and this can also be proved by the UV-vis DRS spectra (Fig. 4). This excellent chemical and mechanical stability of as prepared photocatalyst were critical properties for industrial application in the near future. The immobilization of such pigment sensitized organic-inorganic hybrid photocatalyst is undergoing further investigation in our lab.

### 3.4. Possible photocatalytic mechanism

To the best of our knowledge, efficient photoinduced electron-hole separation and transfer are the key

factors to a photocatalytic reaction; hence it is important and necessary to inhibit the recombination of photoinduced carriers [12]. On the basis of the above experimental studies, a schematic diagram of the band levels of the pigment/TiO<sub>2</sub> composites and the possible reaction mechanism of the photocatalytic procedure are proposed and illustrated in Fig. 7.

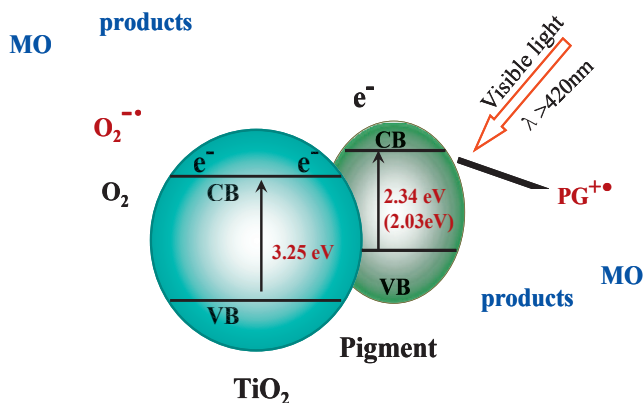


Fig. 7. Schematic diagram of the band levels of pigment/TiO<sub>2</sub> composites and the possible reaction mechanism of the photocatalytic procedure.

Pigment has so narrow band gap energy that it could be irritated easily by visible light and consequently induces the generation of photoelectrons and holes. In fact, pure pigment has poor photoactivity because its narrow band gap energy would result in rapidly recombined for photoelectrons and holes. Meanwhile, TiO<sub>2</sub> possesses both strong electron affinity and high electron conductivity but with a wide energy gap of 3.25 eV, thus it could not be excited by the visible-light irradiation. However, in the case of pigment/TiO<sub>2</sub> heterostructures, we can observe that when pigment are illuminated by photon energy less than 2.95 eV ( $\lambda > 420$  nm), the photoinduced electrons in the reformed conduction band (CB) potential edge on the surface of pigment could easily flow to a lower CB potential edge of TiO<sub>2</sub> [13], thus the recombination of photogenerated electron-hole pairs could be effectively inhibited and the corresponding photocatalytic properties would be greatly improved.

#### 4. Conclusions

This work has shown that the commercial stable pigment (PY and PR) sensitized TiO<sub>2</sub> displaying high visible light photocatalytic activity than original TiO<sub>2</sub> on the degradation of MO. The *TOF* of catalyst for MO based on the content of pigment has nearly loss during the cycle experiment. UV-vis DRS spectra confirmed that the modified catalyst absorbed more photons under visible light irradiation. The research work done thus far suggest that TiO<sub>2</sub> sensitized with small amounts of specific pigment to construct stable organic-inorganic hybrid photocatalytic systems in the heterogeneous photodegradation of organic pollutants has a potential application in wastewater treatment by using solar light or artificial visible light.

#### Acknowledgements

This work was supported by National Natural Science Foundation of China (21103121&21276027), the Doctoral Fund of Ministry of Education of China (20110032120011) and Project of Shandong Province Higher Educational Science and Technology Program (J12L64).

## References

- [1] Linsebigler AL, Guangquan. L, Yates JT. Photocatalysis on TiO<sub>2</sub> surfaces: Principles, mechanisms, and selected results. *Chem. Rev.* 95 (1995)735–758.
- [2] Hoffmann MR, Martin ST, Choi WY, Bahnemann DW. Environmental applications of semiconductor photocatalysis. *Chem. Rev.* 95 (1995) 69–96.
- [3] Alex S, Santhosh U, Das S. Dye sensitization of nanocrystalline TiO<sub>2</sub>: Enhanced efficiency of unsymmetrical versus symmetrical squaraine dyes. *J. Photochem. Photobiol. A: Chem*, 172 (2005) 63–71.
- [4] Chen CC, Ma WH, Zhao JC. Semiconductor-mediated photodegradation of pollutants under visible-light irradiation. *Chem. Soc. Rev.* 39(2010) 4206–4219.
- [5] Lincke G, Molecular stacks as a common characteristic in the crystal lattice of organic pigment dyes: A contribution to the “soluble-insoluble” dichotomy of dyes and pigments from the technological point of view. *Dyes Pigm.* 59 (2003) 1–24.
- [6] Mills A, Hunte SL. An overview of semiconductor photocatalysis. *J. Photochem. Photobiol. A* 108 (1997) 1–35.
- [7] Senthilnathan J, Philip L. Photocatalytic degradation of lindane under UV and visible light using N-doped TiO<sub>2</sub>. *Chem. Eng. J.* 161 (2010) 83–92.
- [8] Zhu YF, Dan Y. Photocatalytic activity of poly(3-hexylthiophene)/titanium dioxide composites for degrading methyl orange. *Sol. Energy Mater. Sol. Cells* 94 (2010) 1658–1664.
- [9] Han H, Bai RB. Highly effective buoyant photocatalyst prepared with a novel layered-TiO<sub>2</sub> configuration on polypropylene fabric and the degradation performance for methyl orange dye under UV–Vis and Vis lights. *Sep. Purif. Technol.* 73 (2010) 142–150.
- [10] Zhu HY, Jiang R, Fu YQ, Guan YJ, Yao J, Xiao L et al. Effective photocatalytic decolorization of methyl orange utilizing TiO<sub>2</sub>/ZnO/chitosan nanocomposite films under simulated solar irradiation. *Desalination* 286 (2012) 41–48.
- [11] Saha S, Pal A, Kundu S, Basu ST, Pal T. Photochemical green synthesis of calcium alginate-stabilized Ag and Au nanoparticles and their catalytic application to 4-nitrophenol reduction. *Langmuir* 26 (2010) 2885–2893.
- [12] Liu Z, Xu XX, Fang JZ, Zhu XM, Chu JH, Li BJ. Microemulsion synthesis, characterization of bismuth oxyiodine/titanium dioxide hybrid nanoparticles with outstanding photocatalytic performance under visible light irradiation. *Appl. Surf. Sci.* 258 (2012) 3771–3778.
- [13] Vinu R, Poliseti S, Madras G.. Dye sensitized visible light degradation of phenolic compounds. *Chem. Eng. J.* 165 (2010) 784–797.